Available online at www.sciencedirect.com
SCIENCE DIRECT®
Polymer 44 (2003) 3641–3647
polymer
www.elsevier.com/locate/polymer

Phase diagram prediction for a blend of Poly(2,6-dimethyl-1,4-phenylene ether) (PPE)/epoxy resin during reaction induced phase separation

Yoshiyuki Ishii[a,1], Anthony J. Ryan[a], Nigel Clarke[b,*]

[a]*Department of Chemistry, The University of Sheffield, Brookhill, Sheffield S3 7HF, UK*
[b]*Department of Chemistry, University of Durham, Durham DH1 3LE, UK*

Received 15 October 2002; received in revised form 27 March 2003; accepted 2 April 2003

Abstract

The phase behavior of a Poly(2,6-dimethyl-1,4-phenylene ether) (PPE)/diglycidyl ether of bisphenol A type epoxy (DGEBA)/diethyltoluenediamine (DETDA) blend during reaction induced phase separation is predicted using Flory–Huggins theory. DGEBA and DETDA are treated as a single pseudo-component in order to reflect the crosslinking polymerisation that occurs between them, and both the PPE and the DGEBA/DETDA pseudo-component are treated as polydisperse. The Flory–Huggins χ parameter was determined by measuring the extent of reaction at the on-set of phase separation for different compositions and temperatures and comparing the results with theory. The χ parameter is then used to determine the coexistence curves as a function of conversion of the DGEBA/DETDA pseudo-component, from which the extent of reaction at which vitrification occurs is predicted. The model is shown to be in good agreement with experimental results.

Keywords: Polymer blends; Phase separation; Glass transition temperature

1. Introduction

In blends of thermoplastics, phase separation is induced by a 'thermal jump' into the immiscible region; such demixing is called 'thermally induced phase separation' [1]. Following a quench into either the metastable or the unstable region of the phase diagram, phase separation will proceed via nucleation and growth or spinodal decomposition [2], respectively. In blends of thermoplastic/thermoset polymers, however, phase separation may also be induced by a 'chemical jump' as the molecular weight of the thermoset increases during cure, and as a consequence the entropy decreases. This demixing process is referred to as 'reaction induced phase separation' or 'chemically induced phase separation'. Again the mechanism of phase separation may be nucleation and growth or spinodal decomposition; the process dictates the morphology development, which is eventually frozen for one of two reasons. Either the gelation of the thermoset and the subsequent formation of an infinite network prevent further phase separation, or the glass transition temperature of one of the phases, which decreases as the cure proceeds, falls below the processing temperature, and vitrification occurs. In the case of the latter, the extent of branching that has taken place has important consequences on the mechanical properties of the blend. In this paper we develop a model to predict the extent of conversion at vitrification for blends in which it is known that vitrification occurs prior to gelation.

Many experimental studies have been performed on systems undergoing reaction-induced phase separation, but due to the complex interaction between phase separation and crosslinking, there have been few theoretical attempts to explain the observations [3–6]. Clarke et al. [7] have utilized the Flory–Huggins theory, which was modified to account for polydispersity by Konigsveld and Staverman [8] and Solc [9], to calculate the phase diagram of a thermoplastic/thermoset blend prior to the gel point. In this treatment, the thermoset was regarded as a polydisperse branched polymer with power law statistics, which is only valid as the gel-point is approached. Since many systems phase separate well before gelation, we extend the model in this paper to include a more realistic model for the molecular weight distribution of the thermoset component,

* Corresponding author.
E-mail address: nigel.clarke@durham.ac.uk (N. Clarke).
[1] Current address: Nanomaterials group, Central Research Laboratory, 2-1 Samejima, Fuji-city Shizuoka 416-8501, Japan.

0032-3861/03/$ - see front matter © 2003 Elsevier Science Ltd. All rights reserved.
doi:10.1016/S0032-3861(03)00294-5

valid during the reaction up to gelation. In addition, in Ref. [7], the thermoplastic component was assumed to be monodisperse. In this paper, we also extend the model to include the complete molecular weight distribution of the thermoplastic.

To quantitatively calculate phase diagrams, it is necessary to estimate the Flory–Huggins χ parameter. Normally, the χ parameter can be determined by fitting the Flory–Huggins equation to a binary phase diagram, which is obtained experimentally. However, it is difficult to measure the phase diagram of a thermoplastic/thermoset blend containing a curing agent, because once heat is applied, the curing reaction will start and the molecular weight distribution of the thermoset will change. Ignoring the curing agent will result in a different parameter. Elliniadis et al. determined the χ parameter of a partially cured epoxy/deuterated-polyarylsulfone/diamine mixture using small angle neutron scattering (SANS) [10]. From the results, the temperature dependence of the phase diagram was obtained for a range of degrees of conversion of the epoxy. Although the χ parameter reflected the contribution of the amine component the use of deuterated samples leads to the possibility of isotopic substitution effects, which are known to alter, in some cases significantly, the phase behaviour of polymer blends.

For thermoplastic/thermoset blends, a more convenient method to determine the χ parameter is from the onset of phase separation. In Fig. 1, we show schematically how the evolution of the phase diagram leads to reaction induced phase separation. If we measure the conversion of the thermoset at the point at which the mixture enters the spinodal region, the χ parameter can be calculated, by determining the corresponding molecular weight distribution of the thermoset, and utilizing an appropriate model, which in this paper is the Flory–Huggins theory.

In a previous paper [11], time-resolved small angle light scattering with DSC was described and the kinetics of phase separation of a Poly(2,6-dimethyl-1,4-phenylene ether)/diglycidyl ether of bisphenol A type epoxy (DGEBA) blend with an aromatic amine hardener was interpreted in terms of the extent of reaction. The conversion at the onset of phase separation was measured. In this paper, the χ parameter is determined using this data and the polydisperse Flory–Huggins model is applied to the mixture to predict the phase behavior during polymerization, and the extent of conversion at vitrification, by using the Fox equation for the glass transition temperature of the blend.

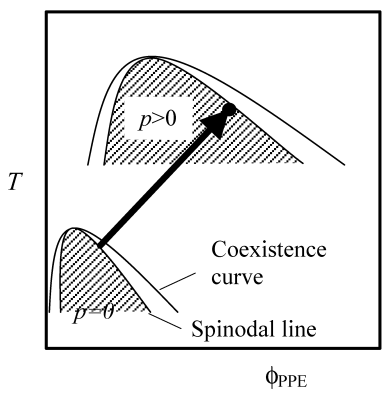

Fig. 1. Schematic representation for the development of the phase diagram during reaction induced phase separation, as a function of p, the conversion and temperature (for a blend that phase separates upon cooling). At a fixed temperature, as p increases, the blend becomes more unstable.

2. Model for phase separation

There are three major assumptions beyond that of the original Flory–Huggins theory, modified by Solc and Konigsveld to account for polydispersity of each component [15].

1. The most significant consequence of the branching process, as far as phase behaviour is concerned, is the wide polydispersity of the branched polymer. The distribution function we use is described in a later section.
2. Each component is chemically stable; i.e. the phase diagrams are calculated assuming the system equilibriates or phase separates fully for each degree of conversion. Physically, this corresponds to assuming that the dynamics of phase separation are faster than the dynamics of crosslinking.
3. The only interaction is between PPE and epoxy/diamine pseudo-monomers; i.e. we treat the DGEBA and the hardener as one component. We also assume that the interaction between components does not change during crosslinking.

The Flory–Huggins free energy of mixing for two polydisperse polymers is [12],

$$\frac{F_{\mathrm{mix}}}{k_{\mathrm{B}}T} = \sum_i \frac{\phi_i}{N_i}\ln\phi_i + \sum_j \frac{\phi_j}{N_j}\ln\phi_j + \chi\left(\sum_i \phi_i\right)\left(\sum_j \phi_j\right) \quad (1)$$

where ϕ_i and N_i are the volume fraction and degree of polymerization of component i of polymer A, and ϕ_j and N_j are the volume fraction and degree of polymerization of component j of polymer B. Note that the conditions of incompressibility, $\sum_i \phi_i = \phi_{\mathrm{A}}$, $\sum_j \phi_j = \phi_{\mathrm{B}}$, and $\phi_{\mathrm{A}} + \phi_{\mathrm{B}} = 1$, are applied throughout. From the Flory–Huggins free energy, Eq. (1), all the properties of the phase diagram are determined as a function of χ. The phase diagram changes as branching proceeds since the molecular weight distribution function of the epoxy/diamine pseudo-component alters with conversion. For each degree of conversion, various features may be determined.

The simplest is the spinodal curve, which represents the

boundary between the mixed state being unstable and metastable. If a blend is taken into the spinodal region phase separation occurs by spinodal decomposition; fluctuations in the composition become unstable and grow rather than decay, as occurs within the one-phase region. It is such fluctuations that are probed by small angle light scattering; thus permitting the spinodal to be accessed experimentally. The experimental results in Ref. [11], i.e. the appearance and growth of a peak in the structure factor, were shown to be consistent with phase separation via spinodal decomposition. Although it has also been shown [13] that in certain circumstances nucleation and growth may also lead to a peak in the structure factor, the measured growth rate of the structure was also shown to be well described by the Cahn–Hilliard theory [14] for spinodal decomposition. Hence we shall assume that this is the phase separation mechanism. The spinodal curve up to the gel point in terms of the molecular weight distribution, which for the epoxy/diamine pseudo-component depends on the degree of branching, can be determined analytically from Eq. (1). It depends only on the weight average degrees of polymerisation, $\bar{N}_{Aw}$ and $\bar{N}_{Bw}$, and is given by,

$$\chi_S = \frac{1}{2}\left(\frac{1}{\phi_A \bar{N}_{Aw}} + \frac{1}{\phi_B \bar{N}_{Bw}}\right) \tag{2}$$

The coexistence curves determine the equilibrium compositions of coexisting phases. Due to the polydispersity of each component, for each blend composition there is a unique set of coexistence curves. They are determined by the condition that the chemical potential of each component is identical in each phase. After a considerable amount of algebra [15], the equations describing the coexistence curves are found to be,

$$1 - \phi''_A - \phi''_B = 0 \tag{3}$$

and

$$\sigma_A(\phi'_A - \phi''_A) + \sigma_B(\phi'_B - \phi''_B) - 2\left(\frac{\phi'_A}{\bar{N}'_{An}} - \frac{\phi''_A}{\bar{N}''_{An}} + \frac{\phi'_B}{\bar{N}'_{Bn}} - \frac{\phi''_B}{\bar{N}''_{Bn}}\right) \tag{4}$$

where ($'$) and ($''$) denote the various properties of the two coexisting phases, σ_A and σ_B are known as separation factors, and represent how much of the higher molecular weight chains of one species has fractionated from the lower molecular weight chains. The coexisting compositions, $\phi'_{A,B}$, $\phi''_{A,B}$, and the number-average degree of polymerisation of each component in each phase, $\bar{N}'_{An,Bn}$, $\bar{N}''_{An,Bn}$, are given by,

$$\phi''_{A,B} = (1+r)\int_0^\infty \frac{\phi_{A,B}(N)}{1 + r\exp\{-\sigma_{A,B}N\}}\mathrm{d}N;$$
$$\phi'_{A,B} = \frac{(1+r)\phi_{A,B} - \phi''_{A,B}}{r} \tag{5}$$

and

$$\bar{N}''_{An,Bn} = \phi''_{A,B}\Big/\left[(1+r)\int_0^\infty \frac{\phi_{A,B}(N)/N}{1 + r\exp\{-\sigma_{A,B}N\}}\mathrm{d}N\right];$$
$$\bar{N}'_{An,Bn} = \frac{(1+r)\bar{N}_{A,B} - \bar{N}''_{A,B}}{r} \tag{6}$$

where $r = \phi'_A - \phi_A/\phi_A - \phi''_A$. In Eqs. (5) and (6) the second relation arises from the condition that the total amount of each polymer, and the overall number-average degree of polymerisation, $\bar{N}_{An,Bn} \equiv \int_0^\infty \phi_{A,B}(N)\mathrm{d}N/\int_0^\infty \times \phi_{A,B}(N)/N\,\mathrm{d}N$, are conserved. Eqs. (3) and (4) are non-linear simultaneous equations which can be solved numerically by fixing r and then determining the corresponding values of σ_A and σ_B, and hence ϕ'_A and ϕ''_A can be found. Once the solution has been found the corresponding value of χ is found from,

$$\chi = \frac{\sigma_A - \sigma_B}{2(\phi'_A - \phi''_A)} \tag{8}$$

3. Molecular weight distribution function

It is evident from the above that in order to be able to predict the familiar temperature-composition phase diagram one needs the molecular weight distribution of PPE and the epoxy/amine pseudocomponent. Furthermore, to predict the evolution of the phase diagram under cure, the molecular weight distribution for the latter at different times during the curing process must be known or modelled.

There are two functions commonly used to describe the polydispersity of linear polymers, the log-normal,

$$\phi_B(N) = k\exp\left\{-\frac{[\log(N/\bar{N}_n) + \sigma^2/2]^2}{2\sigma^2}\right\} \tag{9}$$

and the exponential

$$\phi_B(N) = kN^b\exp(-bN/\bar{N}_n) \tag{10}$$

where $\bar{N}_n \equiv \int_0^\infty \phi(N)\,\mathrm{d}N/\int_0^\infty \phi(N)/N\,\mathrm{d}N$ is the number average degree of polymerization, k is a normalization constant, such that, $\int_0^\infty \phi_B(N)\mathrm{d}N = \phi_B \equiv \phi_{epoxy}$, b and σ determine the higher order moments of the distribution function. (The volume fraction of the epoxy-amine pseudocomponent is denoted by ϕ_{epoxy}.) To fit Eq. (9) or (10) to the data, $\bar{N}_n$ is fixed by the experimental value, whilst $b = 2.232$ and $\sigma^2 = 0.3765$ are chosen to give the correct value of $\bar{N}_w$. Table 1 lists molecular weight averages corresponding to the distribution functions and GPC results for PPE. As can be seen from the data, the log-normal function provides a better approximation, in that the predicted value for, $\bar{N}_z \equiv \int_0^\infty N^2\phi_{A,B}(N)\mathrm{d}N/\int_0^\infty N\phi_{A,B}(N)\,\mathrm{d}N$, the z-average molecular weight, is closer to the experimental value, than that predicted by the exponential

Table 1
Molecular weight averages corresponding to the two distribution functions and the measured GPC results for PPE

		M_n/g mol^{-1}	M_w/g mol^{-1}	M_z/g mol^{-1}
Distribution function	Exponential ($b = 2.232$)	29000	42000	47501
	Log-normal ($\sigma^2 = 0.3765$)	29000	42000	52837
GPC		29000	42000	59000

distribution function. Thus, the log-normal function is used for the following calculations.

We use the Stockmayer model [16] for the volume fraction as a function of degree of polymerisation, N, of a branched polymer arising from an RA_2 (i.e. the epoxy) and RB_f (i.e. the diamine with $f = 4$, to represent the reaction of the two primary amines to epoxy groups, each of which results in a secondary amine, which can also react with an epoxy monomer) polymerisation, which leads to,

$$\phi_A(N) = kN \sum_{n_{min}}^{n_{max}} m(n,s) \tag{11}$$

where k is a normalisation constant, such that $\int_0^\infty \phi_A(N)\,dN = \phi_A \equiv \phi_{PPE}$, ($\phi_{PPE}$ is the overall volume fraction of the thermoplastic). The sum is taken over the number of all n,s-mers in the mixture that have the same total degree of polymerisation, N. If we denote the degree of polymerisation of an RA_2 monomer by g_1, and that of an RB_f monomer by g_2, then for a stoichiometric mixture (such as the experimental system considered in this paper),

$$m(n,s) = \frac{f^{n+1}2^s(1-p)^2(fn-n)!}{p(fn-2n+2-q)!q!n!} \times \left(\frac{p(1-p)^{f-1}}{f(1-p)}\right)^n \left(\frac{p}{2}\right)^s \tag{12}$$

where p is the conversion and,

$$s = \frac{x - g_2 n}{g_1}; \qquad q = s - n + 1 \tag{13}$$

Finally, n_{min} is the smallest integer greater than or equal to,

$$\frac{x-1}{g_1(f-1)+g_2} \tag{14}$$

and n_{max} is the largest integer smaller than or equal to,

$$\frac{x+1}{g_1+g_2} \tag{15}$$

In order to proceed it is essential to assume that $g_1 = g_2$, without such an assumption there is no longer a direct mapping from molecular weight distributions to degree of polymerisation distributions and the problem becomes intractable. For computational purposes, for large n, the summation in Eq. 11 is replaced by an integral with appropriate limits.

4. Experimental

PPE, epoxy (AER 260), and Diethyltoluenediamine-(DETDA) are used as received and were mixed in a Brabender Plastograph Kneader. Details of the materials and blending were described in the previous paper [11].

Time-resolved light scattering with DSC has been used to measure reaction induced phase separation phenomena in-situ. Light scattering gives the onset of phase separation, whereas the Linkam DSC gives enthalpy data and, therefore, the extent of reaction at the onset of phase separation can be deduced. The set-up of the apparatus was also described in a previous paper [11]. As already discussed, we assume that the onset of phase separation as measured by light scattering corresponds to the blend crossing into the spinodal region, hence, the data may be correlated with predictions for the spinodal curve.

The premixed PPE, epoxy, and diethyltoluenediamine were sliced and mounted into DSC pans, which had punched holes, and mica windows were made to establish an optical path. For isothermal measurement, the sample pan was inserted into the DSC stage at room temperature, and the temperature raised rapidly. As soon as the temperature reached the curing temperature, a series of scattering images were taken at approximately 5-second intervals. Fig. 2 shows typical development of scattering intensity and extent of reaction during cure at 195 °C, the extent of reaction at the onset of phase separation is measured as 7.8%, for a mixture containing 50% PPE. Table 2 summarises the results for three compositions cured at two different temperatures.

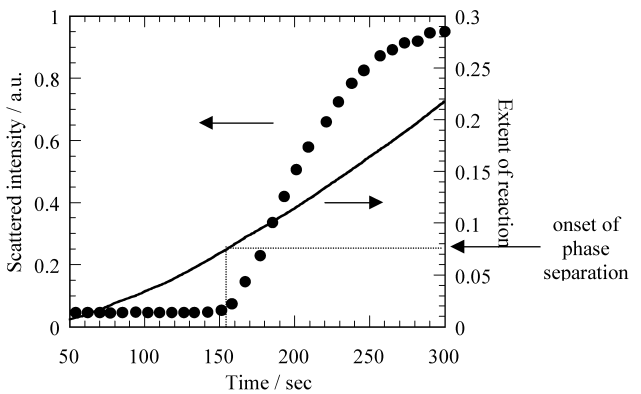

Fig. 2. Onset of phase separation and extent of reaction. The data was taken simultaneously. The blend contains 50 wt% PPE. The curing temperature is 195 °C.

Table 2
Onset of phase separation time and conversion

Isothermal temperature (°C)	PPE content (%)	Onset of phase separation	
		Time (s)	Conversion (%)
175	30	70 ± 5	1.5 ± 0.3
	40	114 ± 5	2.7 ± 0.2
	50	216 ± 5	5.3 ± 0.2
195	30	79 ± 5	2.1 ± 0.4
	40	101 ± 5	4.8 ± 0.4
	50	158 ± 5	7.8 ± 0.4

5. Results and discussion

Preliminary modelling was conducted using the χ parameter determined from the PPE/epoxy phase diagram determined by optical microscopy, DSC, and rheology [11]. However, the resulting fit was poor; the calculated conversion at the temperatures for the onset of phase separation was much higher than the experimental data. This suggests that the χ parameter for the actual ternary mixture system of PPE/epoxy/DETDA is very different from that of the PPE/epoxy blend. Clearly, DETDA affects the phase diagram and we require a better approximation of the effective χ parameter.

As a function of temperature, the spinodal, according to the Flory–Huggins theory, is given by,

$$\chi_S = a + \frac{b}{T} = \frac{1}{2} \times \left(\frac{1}{\phi_{PPE} \bar{N}_{wPPE}} + \frac{1}{(1-\phi_{PPE})\bar{N}_{wepoxy}} \right) \quad (16)$$

where $\bar{N}_{wPPE}$ is the weight average degree of polymerization of the PPE component given by $\bar{N}_{wPPE} = 371$ in this study, and $\bar{N}_{wepoxy}$ is the weight average degree of polymerization of the epoxy/DETDA component. From this equation, if a and b are known for any degree of conversion from which $\bar{N}_{wepoxy}$ can be calculated, the concentration corresponding to the onset of phase separation can be determined. Conversely, if the conversion, as a function of concentration at which phase separation first occurs, is known for a given temperature the above equation can be fitted to determine a and b. Hence, the data obtained from time-resolved small angle light scattering and DSC is used to calculate the temperature dependence of the χ parameter. The degree of polymerisation of the monomer of the epoxy/amine unit is set as $g_1 = g_2 = 3.42$, which was determined by fitting Eq. (2) to the PPE/epoxy binary phase diagram.

The dimensionless χ parameter is thus obtained by using the Stockmayer model to determine the weight average degree of polymerisation for a given conversion. A least-squares fit of Eq. (16) to the data using the two parameters, a and b, and the six data points determined by SALS with DSC as given in Table 2, leads to,

$$\chi = -0.033 + \frac{118}{T} \quad (17)$$

The resultant fit to the data is plotted in Fig. 3 as conversion at onset of phase separation against composition. It is clear that (i) the fit is not particularly good, suggesting that the assumption that either the χ parameter is dependent on the concentration and the extent of reaction, and (ii) that as a consequence the fit predicts that the blend is actually unstable prior to any reaction having taken place for $\phi_{PPE} = 0.3$. Nonetheless, since our principal interest is the behaviour of the mixture much further into the reaction, we shall use Eq. (17) to calculate the phase behaviour for the system. From a physical viewpoint we can imagine that the model corresponds to one of two situations. Firstly, whilst at lower temperatures the initial mixture is unstable, it is mechanically mixed to a homogenous blend prior to curing. Under these circumstances the prediction of the coexistence curves is valid, even for the initial mixture. Secondly, the χ parameter is such that the blend is initially homogenous, but changes during the reaction, our assumption is then that Eq. (17) is valid for the later stages.

As discussed in a previous paper [17], the vitrification of the blend is due to vitrification of the PPE-rich phase and can be estimated simply by the Flory–Huggins theory and Macosko's recursive theory [18]. This point of vitrification of the thermoplastic/thermoset blend is regarded as a Berghmans point [19]. Using the coexistence curves predicted from the model presented in this paper in conjunction with the T_g-composition curves, it is possible to predict the point of vitrification. In Figs. 4–6 we plot the calculated values of the composition of the PPE in the PPE-rich phase at temperatures of 150, 160 and 175 °C, respectively, as a function of conversion. In each case the coexistence composition has been determined for three different bulk PPE compositions. As can be seen, the coexistence composition is only weakly dependent on the

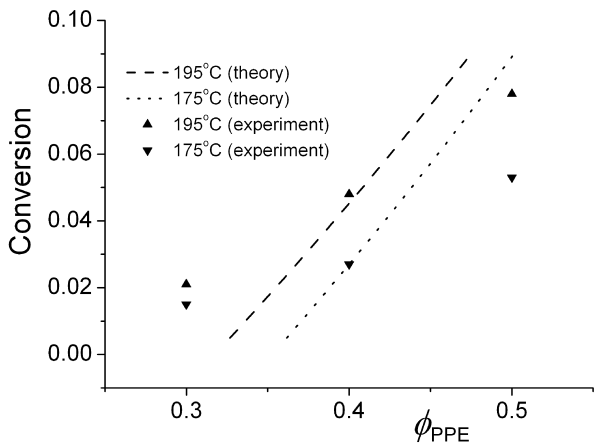

Fig. 3. The conversion at which phase separation occurs, as measured by light scattering, for three different bulk compositions at 175 and 195 °C. The lines show the least-squares fit to the model as discussed in the text.

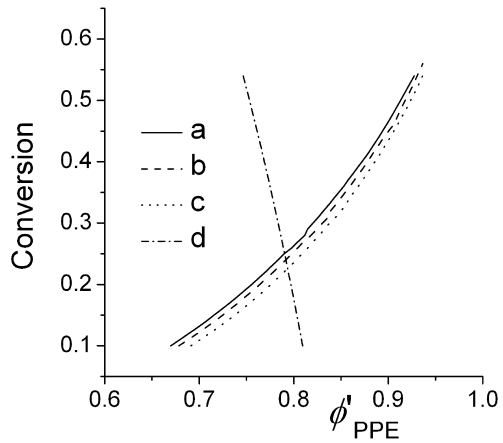

Fig. 4. The coexistence composition of the PPE-rich phase as a function of conversion for three different bulk compositions, (a) $\phi_{PPE} = 0.3$, (b) $\phi_{PPE} = 0.4$ and (c) $\phi_{PPE} = 0.5$, determined using the theory outlined in the text, for $T = 150$ °C. The solid line (d) is the composition, as a function of conversion, at which the glass transition temperature is 150 °C.

bulk composition at these temperatures. This is due to the fact that for the values of conversion shown, the system is deep into the two-phase region of the phase diagram. However, we can see that as the bulk composition of PPE decreases, the coexistence composition at a given conversion also decreases. We have not shown the composition of the epoxy-rich phase since it is indistinguishable from $\phi_{PPE} = 0$, and it is of no interest in determining the point of vitrification. It is the PPE-rich phase that will vitrify first due to the much higher T_g of the PPE at the extent of reaction of interest. In each figure we also plot the composition, as a function of conversion, at which the glass transition temperature is 150, 160 or 175 °C, as appropriate. To determine the T_g line we have used the Fox equation,

$$\frac{1}{T_g} = \frac{\phi'_{PPE}}{T_g^{PPE}} + \frac{1 - \phi'_{PPE}}{T_g^{epoxy}} \tag{18}$$

where ϕ'_{PPE} is the volume fraction of PPE in the PPE-rich phase. The glass transition temperature of the epoxy/amine was determined by using the data shown in Fig. 6 of Ref.

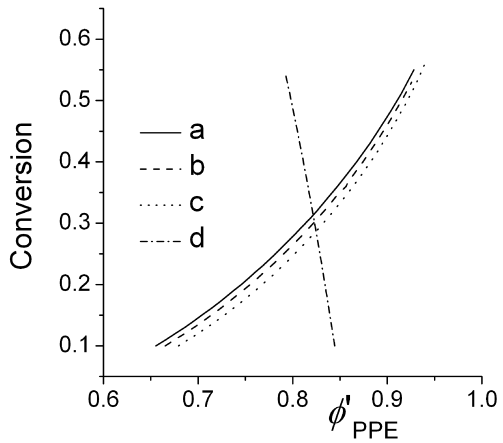

Fig. 5. The same as Fig. 2 except for $T = 160$ °C.

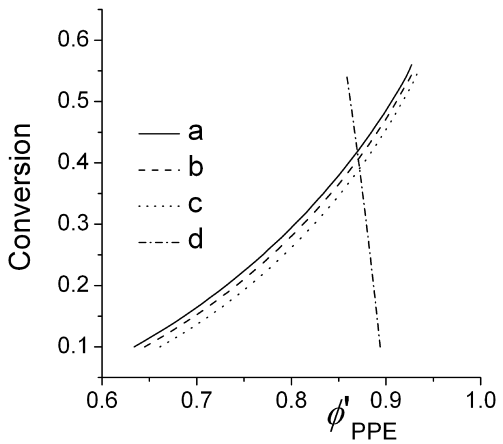

Fig. 6. The same as Fig. 3 except for $T = 175$ °C.

[17]. Hence, the curves labeled *d* in Figs. 4–6, are given by rearranging the above equation as,

$$\phi'_{PPE} = \left(\frac{1}{T_g} - \frac{1}{T_g^{epoxy}(p)}\right) \Big/ \left(\frac{1}{T_g^{PPE}} - \frac{1}{T_g^{epoxy}(p)}\right) \tag{19}$$

The notation $T_g^{epoxy}(p)$ is used to clarify that the glass transition of the epoxy is dependent on p, the extent of reaction. Note that the experimentally determined extent of reaction is the average for the two phases. The point at which this curve intersects the coexistence curve is the Berghmans point for each composition.

In Fig. 7, we show the Berghmans point for three compositions at three different curing temperatures for which experimental data exists. The data corresponds to that first presented in Fig. 11 of Ref. [17]. The qualitative agreement between this aspect of the theory and experiment is excellent, and the quantitative agreement is reasonable given the assumptions made in the model. The conversion at vitrification is predicted and observed to increase as the weight fraction of PPE decreases, there is only a small compositional dependence of the conversion at vitrification

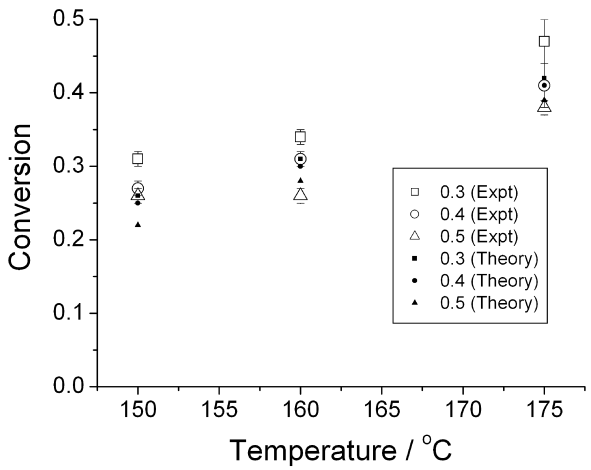

Fig. 7. Comparison of the predicted conversion at vitrification with the experimentally determined values. The error in the experimental measurements range from 0.01 to 0.03 as indicated by the error bars.

at any given temperature, and, since this blend exhibits UCST behaviour, the conversion at vitrification increases as the temperature increases.

6. Conclusions

Using the model first presented in Ref. [7], and extended in this paper to allow for polydispersity of both the thermoplastic and the epoxy/amine pseudocomponent, it is possible to predict the phase diagram of a curing PPE/epoxy/amine blend. In Ref. [7] the molecular weight distribution of the epoxy/amine pseudocomponent was modeled using a power-law distribution which is only valid as the gel-point is approached. Since the blends discussed in this paper phase separate well before the gel-point we have utilized a more realistic distribution function derived by Stockmayer [16], which is valid for the entire reaction process. The χ parameter was determined from time-resolved small angle light scattering with DSC and reflects the nature of the quasi-binary mixture. There are clearly discrepancies between theory and experiment, particularly with regards to the ability of the polydisperse Flory–Huggins model to reproduce the spinodal of the blend at very small values of conversion. The quantitative agreement may be improved if a concentration and extent of reaction dependent χ parameter was used, but this would require further measurements at different temperatures and compositions in order to allow for a reasonable statistical analysis.

Nonetheless, we have shown that modelling has reached a stage where we can make quantitative predictions about the behaviour of these blends. In particular, we can predict phase diagrams as a function of temperature or conversion, and we can determine the conversion at vitrification. The latter as well as being important in dictating properties of the blend, is also a reasonable guide to the time at which vitrification will occur.

Acknowledgements

This research was financially supported by Asahi Chemical (Japan), the University of Sheffield and UMIST. The authors would like to thank R.W. Richards, R. A.L. Jones and S.M. Clarke for their support in the design and N.J. Terrill, C. Lumley and R. Wilkinson for their help in construction, of the time-resolved light scattering.

References

[1] Utracki LA. Polymer Alloys and Blends, Thermodynamics and Rheology. Munich: Carl Hanser Verlag; 1989.
[2] De Gennes PG. Scaling Concepts in Polymer Physics. Ithaca: Cornell University Press; 1979.
[3] Williams RJJ, Rozenberg BA, Pascault JD. Adv Polym Sci 1997;128:95.
[4] Zheng Q, Tan KT, Peng M, Pan Y. J Appl Polym Sci 2002;950:85.
[5] Luo Y, Li H, Li SJ. J Macrmol Sci 2001;1019:38.
[6] Siddhamalli SK, Kyu T. J Appl Polym Sci 2000;1257:77.
[7] Clarke N, McLeish TCB, Jenkins SD. Macromolecules 1995;28:4650.
[8] Konigsveld R, Staverman AJ. J. Polym. Sci., A2 1968;6:325.
[9] Solc K. Macromolecules 1970; 3: 665; 1975; 6: 819.
[10] Elliniadis S, Higgins JS, Clarke N, McLeish TCB, Choudhery RA, Jenkins SD. Polymer 1997;38:4855.
[11] Ishii Y, Ryan AJ. Macromolecules 2000;158:33.
[12] Scot RL, Magat M. J Chem Phys 1945;13:172.
[13] Elicabe GE, Larrondo HA, Williams RJ. J Macromol 1998;31:8173.
[14] Cahn JW, Hilliard JE. J Chem Phys 1958;28:258.
[15] Solc R, Koningsveld R. Coll Czech Chem Commun 1995;60:1689.
[16] Stockmayer WH. J Chem Phys 1943;11:45.
[17] Ishii Y, Ryan AJ. Macromolecules 2000;167:33.
[18] Hale A, Macosko CA, Bair HE. Macromolecules 1991;24:2610.
[19] Arnauts J, Berghmans H. Polym Commun 1987;28:66.